



# Characterization of organic matter in pristine and contaminated coastal marine sediments using solid-state $^{13}\text{C}$ NMR, pyrolytic and thermochemolytic methods: a case study in the San Diego harbor area

Ashish P. Deshmukh <sup>a</sup>, Benny Chefetz <sup>b</sup>, Patrick G. Hatcher <sup>a,b,\*</sup>

<sup>a</sup> Environmental Science Graduate Program, The Ohio State University, 100, W. 18th Ave., Columbus, OH 43210, USA

<sup>b</sup> Department of Chemistry, The Ohio State University, 100, W. 18th Ave., Columbus, OH 43210, USA

Received 26 July 2000; received in revised form 29 March 2001; accepted 6 April 2001

## Abstract

Chemical composition of coastal marine sedimentary organic matter ( $S_D\text{OM}$ ) is a function of natural and anthropogenic inputs to the system. In this study a combination of analytical techniques:  $^{13}\text{C}$  nuclear magnetic resonance (NMR), pyrolysis–gas chromatography/mass spectrometry (Py–GC/MS) and tetramethylammonium hydroxide thermochemolysis–gas chromatography/mass spectrometry (TMAH thermochemolysis–GC/MS) were used to study the contribution of hydrophobic organic contaminants and terrestrial OM to the  $S_D\text{OM}$ . Sediments were collected from two sites in the San Diego Bay: Paleta Creek, which is contaminated, and Coronado Cayes, which is relatively pristine. Concentrations of polycyclic aromatic hydrocarbons (PAHs) at both sites, as determined by ultrasonically assisted lipid extraction are found to be higher in the surface layer, to generally decrease with depth, and to be present at about two orders of magnitude higher concentration at the contaminated site as compared to the pristine site. The sediment samples were partially deashed with HF/HCl treatment before further analysis.  $^{13}\text{C}$ -NMR spectra of the Paleta Creek samples show a higher aromatic carbon content and a distinct phenolic carbon peak. This suggests a large input from terrestrial carbon (lignin). Data from both Py–GC/MS and TMAH thermochemolysis–GC/MS support this and indicate the presence of lignin-derived residues, primarily of the guaiacyl type at the contaminated site. In contrast,  $S_D\text{OM}$  at the Coronado Cayes site exhibits less terrestrial input. In general, the  $S_D\text{OM}$  resembles soil OM rather than typical marine  $S_D\text{OM}$ . Chemical analyses of the lipid-extracted, partially deashed sediments, does not reveal the presence of any PAHs. © 2001 Elsevier Science Ltd. All rights reserved.

**Keywords:** PAHs; Pyrolysis; TMAH; NMR; Lignin; Aromaticity

## 1. Introduction

In marine systems, most of the organic matter (OM) is produced and recycled in the water column by mi-

croorganisms. Degraded and stabilized OM becomes associated with the mineral matter, and becomes part of the sedimentary organic matter ( $S_D\text{OM}$ ). The chemical composition of  $S_D\text{OM}$  may vary with climate, proximity to the shore, and the relative contributions of marine and continental OM residues to the system (Vandenburg et al., 1985).

Compositional analysis of marine  $S_D\text{OM}$  indicates that it consists of 10–15% amino acids, 5–10% carbo-

\* Corresponding author. Tel.: +1-614-688-8799; fax: +1-614-688-4906.

E-mail address: hatcher@chemistry.ohio-state.edu (P.G. Hatcher).

hydrates, 3–5% lignin-derived compounds, and less than 5% lipids (Hedges and Oades, 1997). Most of these constituents can be derived from aquatic and terrestrial sources, but the compounds derived from lignin are solely obtained from terrestrial sources (vascular plants; Hedges and Mann, 1979). Land drainage, and atmospheric input are both important pathways for introduction of terrestrial OM into marine environments. Micro-organisms, primarily bacteria present in marine sediments, mineralize part of the OM to CO<sub>2</sub>, NH<sub>3</sub>, and CH<sub>4</sub>, but the resistant fractions of the OM may remain relatively unaltered. The refractory OM, and the newly formed macromolecules become part of the sedimentary humic substances (HS). The extent of alteration of the OM depends on the distance of the point of sedimentation from the source, depth, oxygen content, particle size, the extent of association with minerals, rate of accumulation, and the extent of bioturbation (Hedges and Oades, 1997). Due to the presence of water, barring the top thin layer (a few millimeters), the sediments are generally depleted of oxygen, and a gradual decrease in the redox-state is seen with depth. Thus, S<sub>D</sub>OM serves as a sink for carbon in modern anoxic environments, since its further mineralization is restricted. Another potential input of OM to S<sub>D</sub>OM is organic contaminants from heavily polluted systems. HS in sediments might play an important role in sorption, immobilization and sequestration of hydrophobic organic contaminants (Carter and Suffet, 1982). Moreover, organic wastes are reported to have a strong effect on the chemical characteristics of HS (Garcia et al., 1994).

Numerous methods have been employed to determine the chemical structural nature of S<sub>D</sub>OM in coastal marine sediments. Cross-polarization magic angle spinning (CPMAS) <sup>13</sup>C-nuclear magnetic resonance (NMR) studies have shown that marine S<sub>D</sub>OM is primarily aliphatic in nature (Hatcher et al., 1980, 1983a). Non-hydrolyzable aliphatic biomacromolecules, which are produced by microalgae (algaenan), exhibit low bioavailability and contribute significantly to S<sub>D</sub>OM (Tegelaar et al., 1989; Gelin et al., 1996). Pyrolysis–gas chromatography/mass spectrometry (Py–GC/MS) studies have shown that S<sub>D</sub>OM contains aliphatic structures associated with carbohydrates, proteins, and carboxylic acid functionalities (Ergin et al., 1996; Peulve et al., 1996; Zegouagh et al., 1999). All these studies suggest that the chemical composition of S<sub>D</sub>OM has a strong relationship with the source of the OM. S<sub>D</sub>OM exhibits higher aliphaticity in systems with higher algal activity, whereas aromaticity is enhanced in cases where a substantial input from terrestrial OM is observed, especially due to the presence of lignin-derived materials.

We report here the use of advanced analytical techniques (<sup>13</sup>C NMR, Py–GC/MS and tetramethylammonium hydroxide thermochemolysis–gas chromatog-

raphy /mass spectrometry (TMAH thermochemolysis–GC/MS)) to study the structural composition of S<sub>D</sub>OM from two sites in San Diego Bay area (contaminated vs. pristine site) in order to determine their source inputs and to eventually evaluate their potential for affecting the nature and distribution of organic contaminants. Analyses of PAHs were also carried out to evaluate the state of contamination for the sediments.

The San Diego Bay area has been the subject of several studies and it has been concluded that it is one of the most contaminated areas (PAHs, polychlorinated biphenyls, and inorganic species such as copper and lead) on the Pacific coast (McCain et al., 1992; Flegal and Sanudo-Wilhelmy, 1993; Coates et al., 1997; Zirino et al., 1998). It has been concluded that the major sources of PAH contamination may be from storm water runoffs from the San Diego International Airport, engine exhausts from ships and recreational boats, and possible oil spills (Zeng and Vista, 1997).

## 2. Materials and methods

### 2.1. Study site

The bay in San Diego is oriented in the southeast–northwest direction. It is over 18 km long, 1–4 km wide, and has a maximum depth of 21 m (Lenihan et al., 1990). The sampling sites were: (i) a contaminated site located in Paleta Creek (latitude 32°40.416'N, longitude 117°06.962'W), and (ii) a relatively pristine site located in Coronado Cayes (latitude 32°38.153'N, longitude 117°08.166'W). The Paleta Creek site is on the Navy's property, and is located near the mouth of a creek that has been impacted, historically, and to a lesser extent currently, by various military and industrial activities.

### 2.2. Sampling

For each sampling site, grab samples were collected from the sediment surface (0–5 cm) and at a depth of 5–25 cm, using a Van Veen grab sampler. Samples were transferred into 1 l sample jars using a stainless steel spoon. Each jar was filled with sediment, capped with seawater, then purged with nitrogen and sealed. Samples were shipped on ice to the laboratory, and stored at 4°C. Immediately upon reaching the laboratory, sub-samples were freeze-dried, ground, and sieved through a 1 mm sieve and stored dry at room temperature. The surface sediment (0–5 cm) samples were designated as Paleta Creek top (PCT), and Coronado Cayes top (CCT). Samples from 5–25 cm depth were designated as Paleta Creek bottom (PCB), and Coronado Cayes bottom (CCB).

### 2.3. Sample preparation

Approximately 25 g of freeze-dried sediment was placed in 250 ml centrifuge tubes, and mixed at 200 rpm with 150 ml of distilled water at room temperature for 2 h. The tubes were centrifuged (4000 rpm for 15 min), and the supernatant was removed carrying with it most of the salts. The sediments were then extracted with 150 ml of dichloromethane:methanol (2:1, v/v) in order to remove lipid-like organic fractions (e.g., organic contaminants). The mixtures were sonicated (pulse mode, 45 s; Branson sonifier 250), and shaken at 200 rpm for 24 h. The tubes were then centrifuged (4000 rpm for 30 min), and the supernatant organic layers were removed. The sediment residues were placed in 1 l plastic bottles and treated with 5% HF and 5% HCl solution for a week, after which the supernatant was decanted and replaced with a freshly prepared HF/HCl solution. This partial deashing procedure was repeated three times. The remaining solids were washed twice with distilled water adjusted to pH 2 with dilute HCl, and freeze-dried (Swift, 1996).

The ash content of the treated samples was measured by loss of weight on ignition at 550°C for 8 h. After partial deashing, the ash content was 46%, 33%, 48% and 62% for the PCT, PCB, CCT and CCB samples, respectively.

### 2.4. PAH analysis

An aliquot of the lipid extract was air-dried. The dry extract was mixed with 100 mg of silica gel (Aldrich, Milwaukee, WI) and hexane and then transferred onto a silica gel column saturated with hexane. Separation of components was performed by elution of hexane followed by benzene (5 ml each). The column effluents (i.e., hexane and benzene fractions) were concentrated and analyzed by high performance liquid chromatography (HPLC).

PAH analysis was performed using HPLC (Waters 2690, Waters, Milford, MA) equipped with a photodiode array detector (Waters 996 PDA detector) and a C-18 reverse-phase column (25 cm×2.1 mm, 50 μm; Supelcosil LC-PAH, Supelco, Bellefonte, PA). An external standard containing 16 PAHs (EPA 610 polynuclear aromatic hydrocarbons mix, Supelco) was used for quantification. Both hexane and benzene fractions were injected onto the HPLC column and PAH concentrations were determined using absorbance at a wavelength of 254 nm. The gradient was 50% acetonitrile and 50% water from time 0 to 30 min, followed by 100% acetonitrile from 30 to 45 min, which was followed by 50% acetonitrile and 50% water from 45 to 50 min. The flow was maintained constant at 0.25 ml/min.

### 2.5. <sup>13</sup>C-NMR spectroscopy

Solid-state CPMAS <sup>13</sup>C-NMR spectra using the ramp-cross-polarization (CP) technique (Hediger et al., 1993) of the HF/HCl treated sediments were obtained with a Bruker 300 MHz NMR-spectrometer (Bruker Analytic GmbH, Germany). The spectrometer operates at a <sup>1</sup>H frequency of 300 MHz and a <sup>13</sup>C frequency of 75 MHz. The following optimized experimental parameters were used: ramp-CP contact time of 2 ms; recycle delay time of 1 s; sweep width of 27 kHz (368 ppm) and line broadening of 150 Hz. Freeze-dried partially deashed samples were placed in a 4 mm rotor, and spun at a frequency of 13 kHz at the magic angle (54.7° to the magnetic field). Contact time of 2 ms was determined to be optimum for all types of carbon functionalities.

The <sup>13</sup>C-NMR spectra were divided into six main regions as defined by Hatcher et al. (1983a, Table 2). The total area attributable to carbohydrates was calculated by summing the area under the peak at 72 ppm (assumed to represent five carbon atoms) and an area equivalent to one carbon atom (i.e., the anomeric carbon atom) from the area of the peak at 109 ppm. The remaining area under the peak at 109 ppm was assumed to be aromatic carbon.

### 2.6. Py-GC/MS

Py-GC/MS was performed on the HF/HCl treated samples, using a Carlo Erba Mega 500 series gas chromatograph (Carlo Erba, Milan, Italy) operating in split mode (20:1), equipped with a CDS Analytical pyroprobe-2000 controller, a CDS AS-2500 pyrolysis autosampler and a 30 m fused silica capillary column coated with chemically bound Rtx-50 (0.25 mm i.d., film thickness 0.25 μm). The interface temperature was held at 273°C. Helium was used as a carrier gas with flow rates of 2 ml min<sup>-1</sup> through the column and 20 ml min<sup>-1</sup> through the split at a head-pressure of 65 kPa. The following oven temperature program was used: initial temperature 40°C (held for 1 min); heating rate 8°C min<sup>-1</sup>; final temperature 320°C (held for 15 min). The gas chromatograph was connected to a Kratos MS-25 RFA mass spectrometer operating at an electron impact potential of at 50 eV with a mass range of 40–510 m/z and a cycle time of 0.7 s (electron beam current 120 μA, source temperature 250°C).

Samples (~0.3 mg) were weighed and transferred onto a minimal amount of silica wool on top of a solid fused silica spacer inside a quartz tube. The tube was dropped by the pyrolysis autosampler into the pyrolysis chamber, which was flushed with the gas prior to pyrolysis, at 70 ml min<sup>-1</sup> for a period of 6 s. After the chamber was automatically connected with the GC column by a six-port valve, the pressure was allowed to equilibrate for 6 s. The pyrolysis

chamber was subsequently heated to 615°C at a rate of 5°C/ms and was held at this temperature for 15 s. After pyrolysis, the chamber was flushed with the carrier gas flow for 21 s. Data acquisition and analysis were performed using a Dart/Kratos Mach 3 data system. Pyrolysis products were identified based on their mass spectra and GC retention times (Van Der Kaaden et al., 1984; Pouwels et al., 1989). The total ion current (TIC) chromatograms of the Py-GC/MS runs were integrated allowing semi-quantitation of the pyrolysis products. Response factors for all compounds produced upon pyrolysis were assumed to be equal to 1.

### 2.7. TMAH thermochemolysis–GC/MS

Freeze-dried HF/HCl treated sediment samples (2–5 mg) were weighed and placed in glass tubes with 200 µl of TMAH (25% wet in methanol; Aldrich). The methanol was evaporated under a stream of nitrogen. The tubes were sealed under vacuum, and subsequently placed in an oven at 250°C for 30 min. After cooling, the tubes were cracked open, internal standard (1951 ng of *n*-eicosane) was added and the inside surfaces of the tubes were extracted (three times) using ethyl acetate. The combined extracts were reduced to approximately 50 µl under a stream of N<sub>2</sub>. Gas chromatographic analyses were performed using a Hewlett-Packard 7683 gas chromatograph (Hewlett Packard, Palo Alto, CA), equipped with a 15 m fused silica capillary column coated with chemically bound DB-5 (0.25 mm i.d., film thickness 0.1 µm; Supelco, Bellefonte, PA). Samples (1 µl) were injected using an autoinjector (Hewlett-Packard 6890 series), with a split ratio of 5 and an inlet temperature of 310°C. Helium was used as carrier gas with a flow rate of 1 ml/min; electronic flow control was

set for constant flow. The gas chromatographic oven temperature was programmed from 40–300°C at the rate of 8°C min<sup>-1</sup>. The GC was directly coupled to a Pegasus II (Leco® Corporation, St. Joseph, MI) time-of-flight mass spectrometer by a deactivated fused silica transfer-line heated to 300°C. Mass spectra from 33 to 700 m/z were accumulated at a scan rate of 2 kHz, summed and recorded at 9 scans/s. Most peaks were assigned by comparison with the National Institute of Standards and Technology library (NIST, version 1.6).

## 3. Results

### 3.1. PAH analysis

The PAHs analyses (Table 1) indicate that the Paleta Creek site is contaminated with individual PAH concentrations between 0.4–413 µg kg<sup>-1</sup>, whereas the Coronado Cayes site has much lower concentrations (0.1–1.7 µg kg<sup>-1</sup>). In general, the PAH concentrations were higher in the surface layer as compared to the subsurface layer. In the Paleta Creek samples, the PAHs with the highest concentrations had high molecular weights with more than four fused benzene rings (benzo(e)acephenanthylene, benzo(k)fluoranthene, chrysene, benzo(a)pyrene, benzo(g,h,i)perylene and indeno(1,2,3-c,d)pyrene).

### 3.2. <sup>13</sup>C-NMR spectroscopy

The CPMAS <sup>13</sup>C-NMR technique provides useful information about the general macromolecular structure of S<sub>p</sub>OM (Hatcher et al., 1983a). The <sup>13</sup>C-NMR spectra of the HF-treated sediment samples are presented in Fig. 1. All spectra exhibited similar peaks at 30 ppm

Table 1  
Concentration of PAHs in the San Diego Bay sediments (µg kg<sup>-1</sup>±S.D.)

| Sample                   | Concentration (µg kg <sup>-1</sup> ) |            |         |         |
|--------------------------|--------------------------------------|------------|---------|---------|
|                          | PCT                                  | PCB        | CCT     | CCB     |
| Fluorene                 | 0.4±0.2                              | 0.5±0      | n.d.    | n.d.    |
| Phenanthrene             | 22.1±11.3                            | 8.4±2.2    | 1.7±0.4 | 0.5±0.1 |
| Anthracene               | 5.7±4.2                              | 3.4±2.6    | n.d.    | 0.1±0   |
| Fluoranthene             | 152.7±11.3                           | 15.8±1.7   | 1.2±0.2 | 0.4±0.1 |
| Pyrene                   | 15.4±9.0                             | 42.9±17.5  | 0.6±0.4 | 0.4±0.1 |
| Benzo(a)anthracene       | 75.8±28.3                            | 28.8±3.2   | 0.1±0   | n.d.    |
| Chrysene                 | 347.3±64.5                           | 167.3±18.9 | 1.6±0   | n.d.    |
| Benzo(e)acephenanthylene | 413.0±54.1                           | 188.3±14.0 | 0.1±0   | n.d.    |
| Benzo(k)fluoranthene     | 385.3±106.1                          | 3.3±0.4    | 0.4±0   | n.d.    |
| Benzo(a)pyrene           | 248.1±56.9                           | 153.5±5.8  | 0.5±0.2 | n.d.    |
| Dibenz(a,h)anthracene    | 4.6±0                                | 9.3±0.2    | n.d.    | n.d.    |
| Benzo(g,h,i)perylene     | 334.3±85.6                           | 253.3±16.7 | 1.2±0.1 | 0.5±0.2 |
| Indeno(1,2,3-cd)pyrene   | 233.7±56.9                           | 64.9±73.7  | 0.7±0.3 | 0.2±0.1 |

n.d. = Not detected.

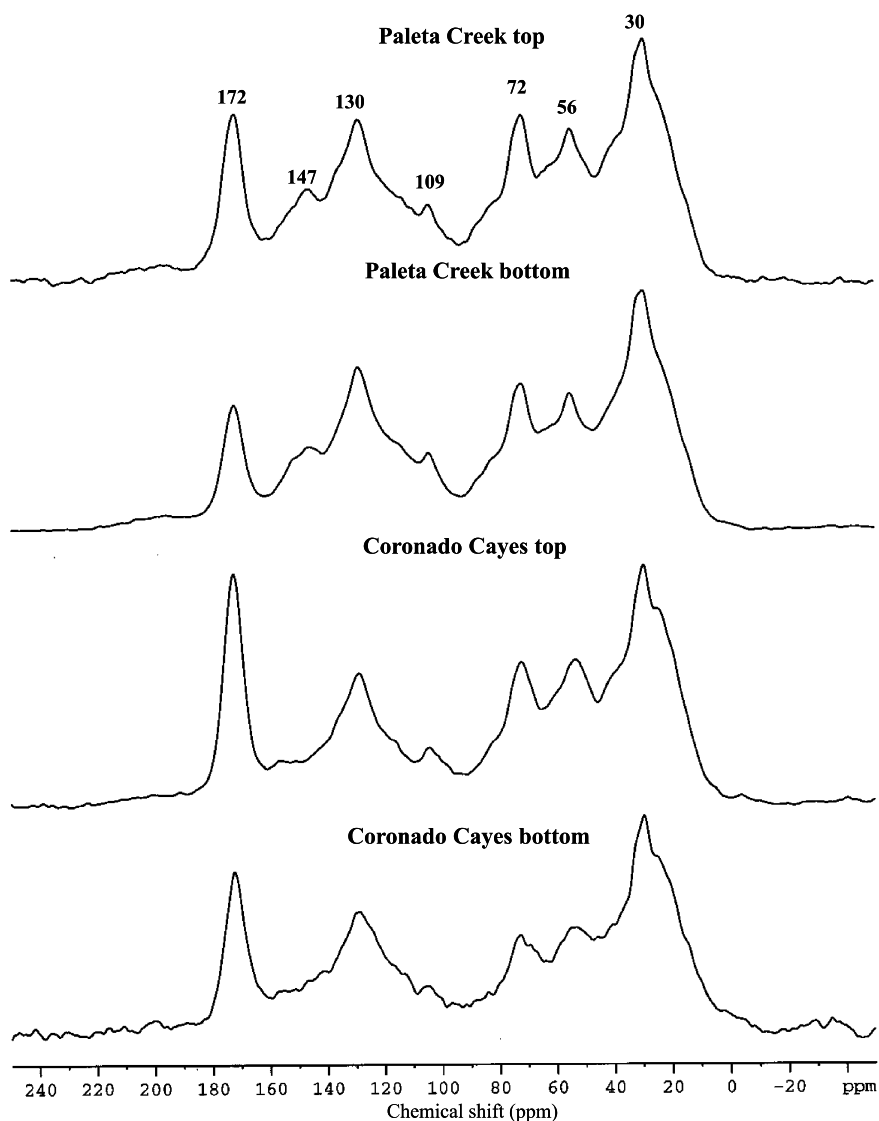


Fig. 1. CPMAS  $^{13}\text{C}$ -NMR spectra of the partially deashed sediments.

(paraffinic carbon), 56 ppm (methoxy carbon), 72 ppm (alkyl-O carbon), 109 ppm (anomeric carbon of carbohydrates plus aromatic carbons), a shoulder at 115 ppm (H-substituted aromatic carbon), 130 ppm (C-substituted aromatic carbon), 147 ppm (O-substituted aromatic carbon), 172 ppm (carboxyl, ester or amide carbon), and a broad poorly resolved peak between 190 and 220 ppm (ketone and aldehyde carbon). The major carbon-containing groups were: (i) the paraffinic carbon (which represents 29–35% of the total carbon), (ii) carbohydrates (which represent 13–17% of the total carbon); and (iii) the aromatic carbon (which represents 23–30% of the total carbon; Table 2). Although the  $^{13}\text{C}$ -NMR spectra obtained for all four samples displayed

similar general shapes, certain differences could be noticed: (i) spectra of samples from surface layers at both sites, exhibited higher carboxyl, methoxyl, and carbohydrate carbon content as compared to the spectra of samples from subsurface layers; (ii) spectra obtained from the Paleta Creek samples exhibited higher aromatic carbon content, whereas those from the pristine site had a relatively higher aliphatic content; (iii) a well-formed peak at 147 ppm (aryl-O of phenolic and methoxy phenolic groups) was observed only in the NMR spectra of the Paleta Creek samples; and (iv) the spectra obtained for the Coronado Cayes samples exhibited a significantly higher carboxyl/amide content (12–14%), compared to those for the Paleta Creek samples

Table 2

Distribution of different C-containing groups in the partially deashed San Diego Bay sediments as determined by CPMAS  $^{13}\text{C}$ -NMR (percent of total carbon)

| Chemical shift (ppm) | C-containing group |          |              |          |                |          |
|----------------------|--------------------|----------|--------------|----------|----------------|----------|
|                      | Aliphatic          | Methoxyl | Carbohydrate | Aromatic | Carboxyl/amide | Carbonyl |
|                      | 0–50               | 50–60    | 60–112       | 112–160  | 160–190        | 190–220  |
| <i>Sample</i>        |                    |          |              |          |                |          |
| PCT                  | 29.0               | 13.3     | 16.7         | 28.7     | 10.5           | 1.9      |
| PCB                  | 30.7               | 12.9     | 16.2         | 30.1     | 8.6            | 1.6      |
| CCT                  | 32.3               | 14.1     | 15.5         | 22.6     | 14.1           | 1.4      |
| CCB                  | 35.2               | 12.5     | 13.0         | 26.2     | 12.2           | 0.9      |

(8–10%), with surface sediments being richer in such groups than bottom sediments.

### 3.3. Py-GC/MS

TIC chromatograms of the Py-GC/MS analysis of the Paleta Creek, and Coronado Cayes samples are presented in Figs. 2 and 3, respectively. The main compounds identified in the chromatograms were grouped

into five major classes of compounds: polysaccharides (PS), proteins (PR), lignin-derived compounds (LG), alkanes/alkenes (AL) and fatty acids (FA; Table 3). Compounds that could not be assigned to a single biological source (such as several derivatives of benzene, thiophene, and non-lignin phenols) were classified as unassigned (US). In general, the level of *n*-alkenes was higher than that of the corresponding *n*-alkanes in all four samples.

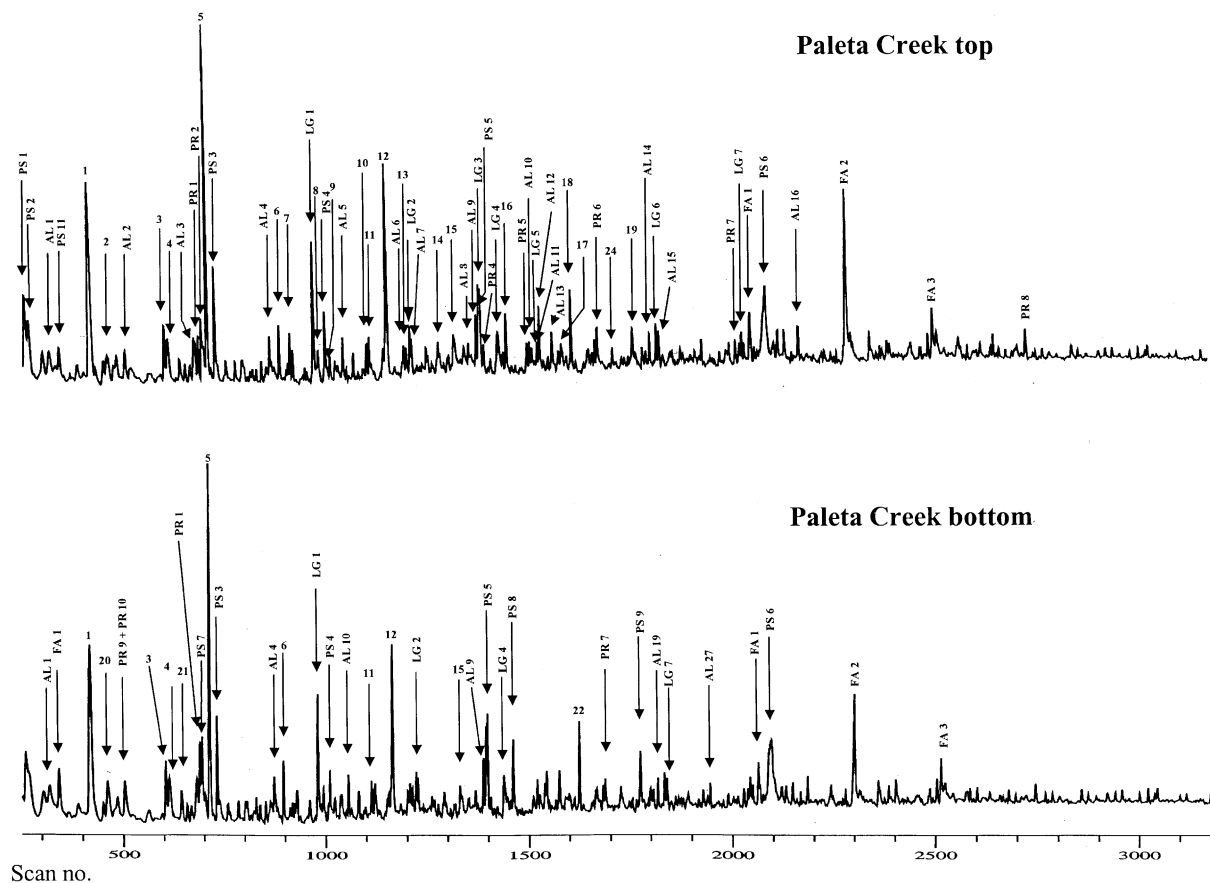


Fig. 2. Py-GC/MS chromatograms of the partially deashed Paleta Creek sediment samples.

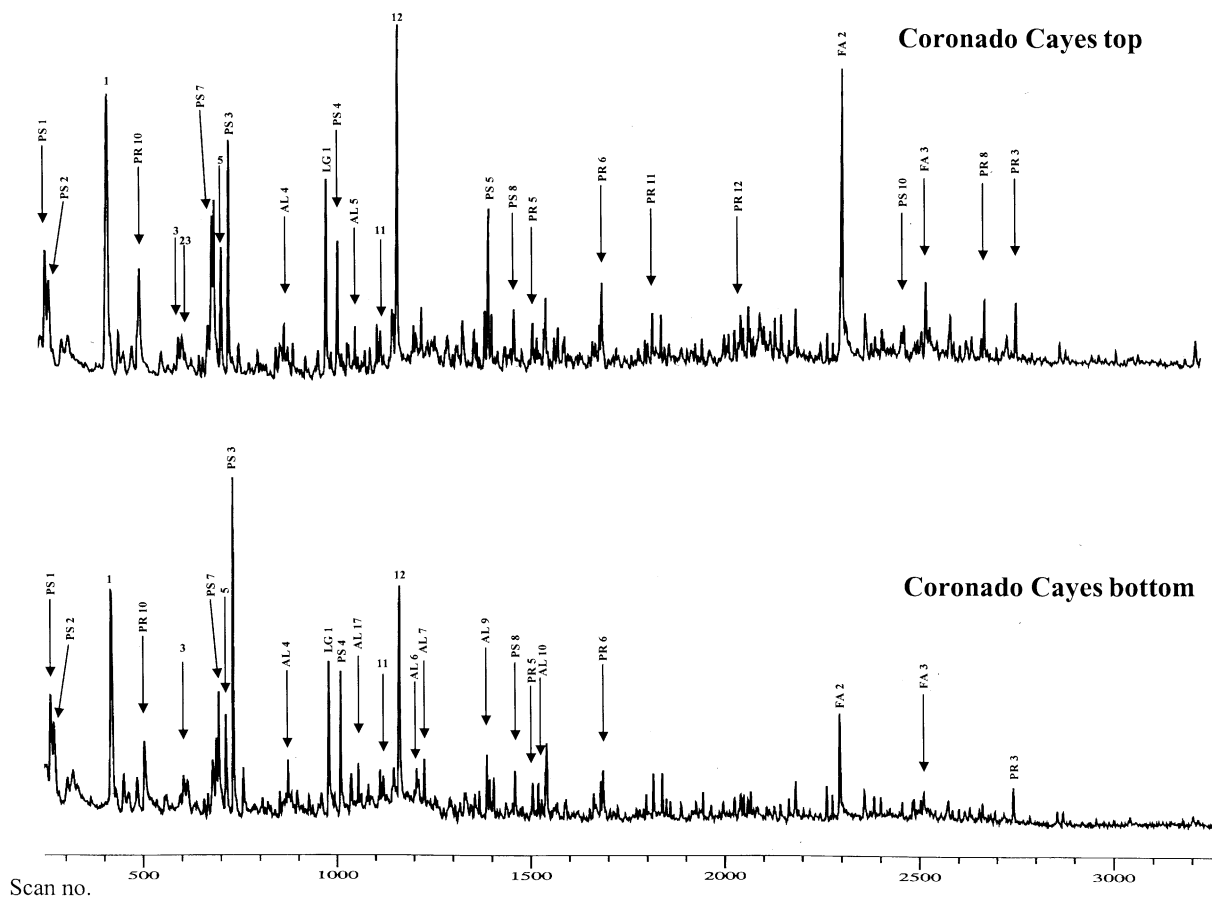


Fig. 3. Py-GC/MS chromatograms of the partially deashed Coronado Cayes sediment samples.

The Py-GC/MS chromatograms recorded for the Paleta Creek samples exhibited the following major peaks: PS-derived, 2- and 3-methyl butanal, 2-furan-carboxaldehyde and 5-methyl-2-furancarboxaldehyde; PR-derived, 4-imidazoline-2-one, 1H-indene, 2,5-pyrrolidinedione and 1H-indole; and LG-derived, phenol, 2-methoxyphenol, 2-methoxy-4-methyl phenol, 1,2-benzenediol and 2-methoxy-4-(1-propenyl) phenol. The major FA peaks were C<sub>14</sub>, C<sub>16</sub>, C<sub>18</sub>, and the major unassigned compounds were toluene, styrene, 3-methyl phenol, and 5-methyl-2-(1-methylethyl) phenol.

The Py-GC/MS chromatograms recorded for the Coronado Cayes samples exhibited the following major peaks: PS-derived, 2- and 3-methyl butanal, 2-furan-methanol, 2-furancarboxaldehyde, 5-methyl-2-furancarboxaldehyde and 2,3-dihydrobenzofuran; and PR-derived, pyrrole, 2-methyl pyrrole, 4-imidazoline-2-one, 1H-indene, 2,5-pyrrolidinedione, 1H-indole and 2-methyl indole. The only LG-derived peak detected was phenol. The major FA peaks were C<sub>14</sub>, C<sub>16</sub>, C<sub>18</sub>, and the main US peaks were toluene, styrene and 3-methyl phenol.

The major differences between the samples were: (i) the styrene peaks were more dominant in the pyrolysis chromatograms of the Paleta Creek samples as compared to the Coronado Cayes chromatograms; (ii) the 3-methyl phenol peak was larger in the Coronado Cayes chromatograms as compared to the Paleta Creek chromatograms; (iii) the C<sub>16</sub> FA peak was more pronounced in the surface layer chromatograms (PCT and CCT) than subsurface layers (PCB and CCB); and (iv) levoglucosan (PS 6) was identified only in the Paleta Creek chromatograms.

Semi-quantitative data calculated from the Py-GC/MS chromatograms is presented in Table 4. The main differences between the samples were: (i) PCT sample exhibited lower levels of PS- and PR-derived compounds, but higher levels of LG-derived compounds and FA when compared to the PCB sample; (ii) the CCT sample exhibited higher levels of PR-derived compounds and FA, but lower levels of PS and LG-derived compounds as compared to the CCB sample; and (iii) the Coronado Cayes samples exhibited a higher level of PS-derived compounds, and a lower level of AL and

Table 3  
Peak identification of Py–GC/MS products obtained from the San Diego Bay sediment samples

| <i>Compounds derived from polysaccharide structures</i> |   |
|---|---|
| PS 1  | 3-Methyl butanal                                      |
| PS 2  | 2-Methyl butanal                                      |
| PS 3  | 2-Furancarboxaldehyde                                 |
| PS 4  | 5-Methyl,2-furancarboxaldehyde                        |
| PS 5  | 2-Furanmethanol                                       |
| PS 6  | Levoglucofan  |
| PS 7  | 2,3-Dihydro-3-furanone                                |
| PS 8  | 2,3-Dihydrobenzofuran                                 |
| PS 9  | 1,3-Isobenzofurandione                                |
| PS 10   | Amino sugar   |
| <i>Compounds derived from protein structures</i>        |   |
| PR 1  | 2-Methyl pyrrole                                      |
| PR 2  | 4-Imidazoline-2-one                                   |
| PR 3  | 5H, 10H-dipyrrolo [1,2-a:1',2'-d] pyrazine-5,10-dione |
| PR 4  | Benzeneacetone  |
| PR 5  | 2,5-Pyrrolidenedione                                  |
| PR 6  | 1H-Indole   |
| PR 7  | 1H-Isoindole-1,3(2H)-dione                            |
| PR 8  | Hexadecanamide  |
| PR 9  | Pyridine  |
| PR 10   | Pyrrole   |
| PR 11   | 3-Methyl indole                                       |
| PR 12   | 2,3-Dihydro-4-methyl indole                           |
| <i>Compounds derived from lignin structures</i>         |   |
| LG 1  | Phenol  |
| LG 2  | 2-Methoxyphenol                                       |
| LG 3  | 2-Methoxy-4-methyl phenol                             |
| LG 4  | 1,2-Benzenediol                                       |
| LG 5  | 4-Ethyl-2-methoxy phenol                              |
| LG 6  | 2-Methoxy, 4-(1-propenyl) phenol                      |
| LG 7  | 1-(4-hydroxy-3-methoxyphenyl) 2-propanone             |
| <i>Alkanes and alkenes</i>                              |   |
| AL 1  | 1-Octene  |
| AL 2  | 3-Ethyl cyclopentene                                  |
| AL 3  | 1-Decene  |
| AL 4  | 1-Undecene  |
| AL 5  | 1-Dodecene  |
| AL 6  | Tridecane   |
| AL 7  | 1-Tridecene   |
| AL 8  | Tetradecane   |
| AL 9  | 1-Tetradecene   |
| AL 10   | Pentadecane   |
| AL 11   | 1-Pentadecene   |
| AL 12   | Branched alkane                                       |
| AL 13   | Branched alkane                                       |
| AL 14   | 1-Heptadecene   |
| AL 15   | 2-Isohexyl-6-methyl-1-heptene                         |
| AL 16   | 1-Eicosene  |
| <i>Fatty acids</i>                                      |   |
| FA 1  | Tetradecanoic acid                                    |
| FA 2  | Hexadecanoic acid                                     |
| FA 3  | Octadecanoic acid                                     |

Table 3 (continued)

| <i>Unassigned compounds</i> |                                    |
|-----------------------------|------------------------------------|
| 1                           | Toluene                            |
| 2                           | 2-Methyl thiophene                 |
| 3                           | Ethyl benzene                      |
| 4                           | 1,4-Dimethyl benzene               |
| 5                           | Styrene                            |
| 6                           | 1-Methyl ethenyl benzene           |
| 7                           | 1-Propenyl benzene                 |
| 8                           | 1-Ethenyl 2-methyl benzene         |
| 9                           | 2-Propenyl benzene                 |
| 10                          | 1,3-Dihydroxybenzene               |
| 11                          | 2-Methylphenol                     |
| 12                          | 3-Methyl phenol                    |
| 13                          | 1,2,4,5-Tetramethylbenzene         |
| 14                          | 2,4-Dimethyl phenol                |
| 15                          | 3-Ethyl phenol                     |
| 16                          | 2-Methylbenzaldehyde               |
| 17                          | 3-Methyl 1,2-benzenediol           |
| 18                          | 5-Methyl-2-(1-methylethyl) phenol  |
| 19                          | Benzene-1,2-dicarboxylic acid      |
| 20                          | 3-Methyl thiophene                 |
| 21                          | 2,5-Dimethyl thiophene             |
| 22                          | 1,3-Diamino 2,4,6-trimethylbenzene |
| 23                          | 1,3-Dimethylbenzene                |
| 24                          | 1,1'-Biphenyl                      |

LG-derived structures as compared to the Paleta Creek samples.

### 3.4. TMAH thermochemolysis–GC/MS

Thermochemolysis in the presence of TMAH is a highly selective technique for cleaving ester and certain ether linkages in macromolecular OM (Hatcher et al., 1996). This technique has been used to characterize lignin (Clifford et al., 1995), HS (Hatcher and Clifford, 1994), coalified woods (McKinney and Hatcher, 1996), carbohydrates (Fabbri and Helleur, 1999), lipids (Challinor, 1996), cutan (McKinney et al., 1996), and cutin (del Rio et al., 1998), marine sediments (Pulchan et al., 1997), and composted OM (Chefetz et al., 2000). This technique is shown to provide additional information on the structure and composition of macromolecules. It has been demonstrated that the TMAH technique is a chemolytic procedure that hydrolyzes and methylates ester and ether linkages, assisting depolymerization and methylation of lignin (Filley et al., 1999).

The TMAH thermochemolysis–GC/MS chromatograms of the sediment samples were dominated by fatty acid methyl esters (FAMES), methylated LG, methylated mono and dicarboxylic acids, non-lignin aromatic structures, and heterocyclic nitrogen compounds (Figs. 4 and 5). Identification of these peaks is listed in Table 5. The main peaks obtained in the Paleta Creek chromatograms were G1, G3, G4, G5, G6, G10, G21, G22, P3,

Table 4

Distribution of polysaccharide-, protein-, and lignin-derived, and alkane/alkene-, fatty acid pyrolysis products in the San Diego Bay sediments as calculated from the TIC chromatograms of Py-GC/MS

| Sample | PS <sup>a</sup> | PR <sup>b</sup> | LG <sup>c</sup> | AL <sup>d</sup> | FA <sup>e</sup> |
|--------|-----------------|-----------------|-----------------|-----------------|-----------------|
| PCT    | 14.9            | 6.6             | 10.0            | 15.3            | 10.9            |
| PCB    | 20.3            | 8.6             | 5.5             | 3.5             | 7.8             |
| CCT    | 35.5            | 9.2             | 5.2             | 0.4             | 12.4            |
| CCB    | 45.3            | 6.2             | 7.2             | 0.1             | 4.7             |

<sup>a</sup> PS = Polysaccharide.

<sup>b</sup> PR = Protein.

<sup>c</sup> LG = Lignin.

<sup>d</sup> Alkanes/alkenes.

<sup>e</sup> FA = Fatty acids.

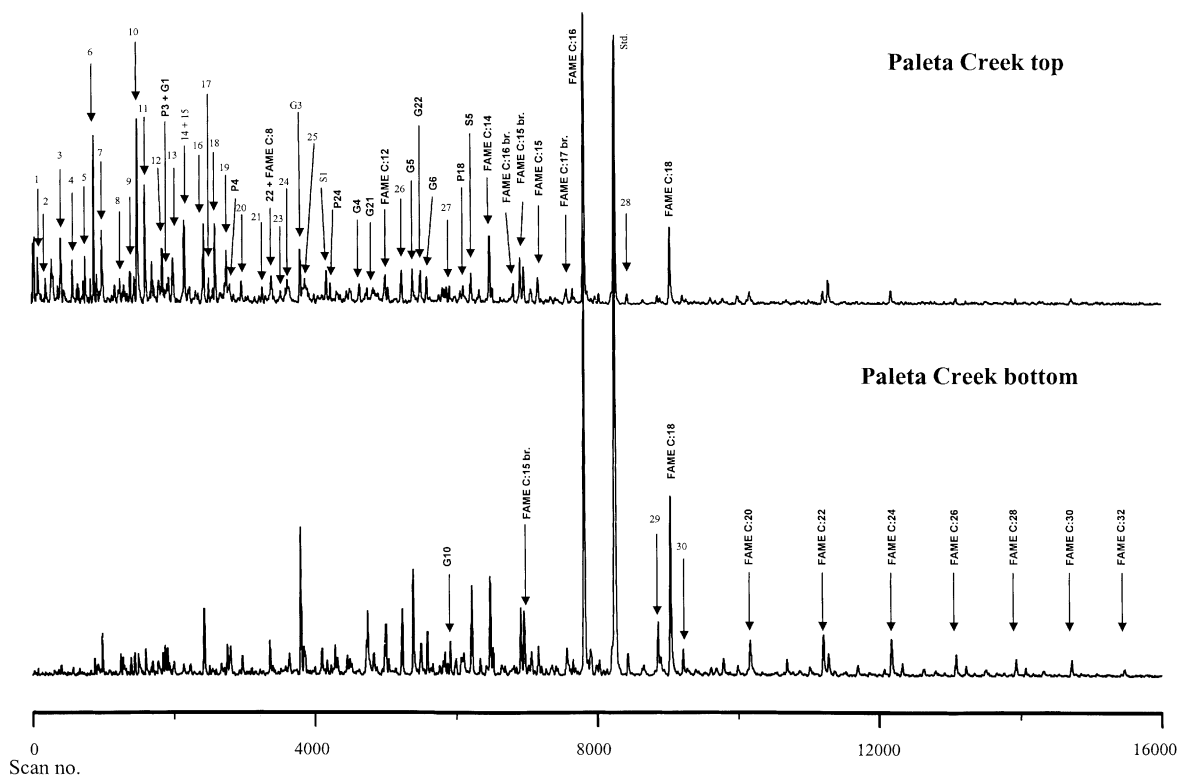


Fig. 4. TMAH thermochemolysis-GC/MS chromatograms of the partially deashed Paleta Creek sediment samples.

P4, P18, P24, S1 and S5 (lignin-derived); C<sub>12</sub>–C<sub>32</sub> FAMES; C<sub>4</sub>–C<sub>9</sub> dicarboxylic acid methylesters (DAMES); and 1-methyl-2,5-pyrrolidinedione, 1-piperidincarboxaldehyde, 1,2,6-trimethyl-4(1H)-pyridinone and 3-ethyl-2,6-piperidinedione (N-containing heterocycles). The major products obtained from the TMAH thermochemolysis of the Coronado Cayes samples were G3, P18 and P4 (lignin-derived); C<sub>12</sub>–C<sub>24</sub> FAMES; C<sub>4</sub>–C<sub>5</sub> DAMES; and 1-methyl-2,5-pyrrolidinedione and 2-methyl-1H-isindole-1,3-dione (N-containing heterocycles).

The major differences between the chromatograms were: (i) while even-numbered FAMES (C<sub>12</sub>–C<sub>24</sub>) were more pronounced in the surface sample than in the subsurface sample in the Coronado Cayes site, the opposite trend was observed in the Paleta Creek samples; (ii) the Coronado Cayes chromatograms exhibited a higher level of the C<sub>4</sub> and C<sub>5</sub> DAMES than the Paleta Creek samples; (iii) the lignin-derived peaks were significantly more dominant in the samples from the Paleta Creek than the Coronado Cayes site; and (iv) protein-derived compounds such as pyrroles, pyrrolidinediones,

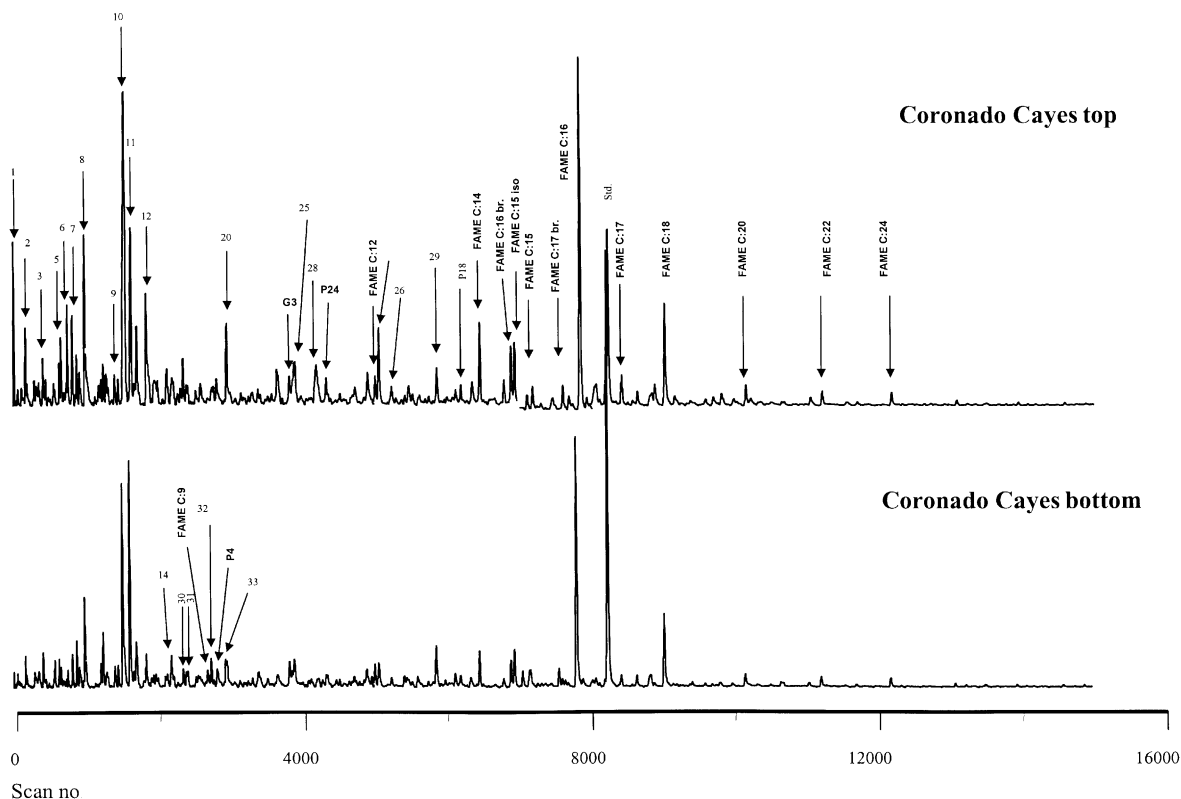


Fig. 5. TMAH thermochemolysis-GC/MS chromatograms of the partially deashed Coronado Cayes sediment samples.

and piperidinediones were more abundant in the surface chromatograms as compared to the subsurface samples.

#### 4. Discussion

In this study we have applied a combination of advanced analytical techniques ( $^{13}\text{C}$ -NMR, Py-GC/MS, and TMAH thermochemolysis-GC/MS) to study the nature of the bulk  $\text{S}_\text{D}$ OM macromolecules from marine sediments associated with contaminated OM. Two sites were studied: Paleta Creek (a contaminated site) and a relatively pristine site (Coronado Cayes). The Paleta Creek site is on the Navy's property, and is located near the mouth of a creek that has been impacted, historically, and to a lesser extent currently, by various military and industrial activities. Sediments from this site are characterized by high PAH concentration (total PAH concentration was  $940\text{--}2300\ \mu\text{g kg}^{-1}$ ). Samples from the pristine site exhibited a significantly lower concentration of PAHs (total PAH concentration was  $2\text{--}8\ \mu\text{g kg}^{-1}$ ). In a study of sediments from Baltimore Harbor, total PAH concentrations varied from  $90$  to  $46\,200\ \mu\text{g kg}^{-1}$  (Ashley and Baker, 1999). It was found that there was tremendous spatial variability and that there was no correlation

between concentration and organic carbon content or grain size. Proximity to sources such as urban stormwater runoff discharge, discharges from steel plant (pyrolysis of coal) resulted in higher concentrations of PAHs. Due to their low water solubilities and higher affinity for OM, the higher molecular weight PAHs were concentrated closer to their source, whereas the low molecular weight compounds traveled further distances. In a similar study conducted on sediments from Xiamen Harbor, China, total PAH concentrations in surficial sediments were found to be  $247\text{--}480\ \mu\text{g kg}^{-1}$  dry weight (Zhou et al., 2000). This site received discharge from municipal wastewater, input from harbor and maricultural activities, and also had petroleum contamination. PAHs in this area were dominated by phenanthrene (from petroleum contamination), and indeno (1,2,3-cd) pyrene (pyrolytic). The Elizabeth River in Norfolk, VA is a highly industrialized estuary bordered by the cities of Norfolk and Portsmouth, VA. The system has been contaminated by creosote, which was used for wood treatment in factories located along the river. The total PAH concentration varied with location with a maximum concentration of  $15\,000\,000\ \mu\text{g kg}^{-1}$ . However, in this case the low molecular weight PAHs, which are derived from creosote, were seen to be dominating (Huggett et al., 1992).

Table 5  
Peak identification of TMAH thermochemolysis–GC/MS products of the San Diego Bay sediments

| <i>Lignin-derived peaks</i>  |   |
|--|---|
| G1   | 1,2-Dimethoxybenzene                                    |
| G3   | 4-Ethenyl-1,2-dimethoxy-benzene                         |
| G4   | 3,4-Dimethoxy-benzaldehyde                              |
| G5   | 3,4-Dimethoxy acetophenone                              |
| G6   | Benzoic acid, 3,4-dimethoxy-, methyl ester              |
| G10  | <i>cis</i> -1-(3,4-dimethoxyphenyl)-1-methoxy-1-propene |
| G21  | 1,2-Dimethoxy-4-(1-propenyl)-benzene,                   |
| G22  | 1-(3,4-dimethoxyphenyl)-2-propanone                     |
| P3   | 1-Ethenyl-4-methoxy-benzene                             |
| P4   | 4-Methoxy-benzaldehyde                                  |
| P18  | <i>trans</i> -Methyl (4-methoxy) cinnamate              |
| P24  | Benzenecetic acid, 4-methoxy-, methyl ester             |
| S1   | 1,2,3-Trimethoxybenzene                                 |
| S5   | 3,4,5-Trimethoxyphenyl ethanone                         |
| <i>Monocarboxylic-, dicarboxylic-, and fatty acid-methyl ester peaks</i> |   |
| 2  | 2-Methoxy-3-methyl-butyric acid, methyl ester           |
| 5  | Propanoic acid, 2-methyl-, anhydride                    |
| 6  | Propanoic acid, 2-(methylthio)-, methyl ester           |
| 7  | Butanedioic acid, dimethyl ester                        |
| 8  | Butanedioic acid, methyl-, dimethyl ester               |
| 12   | Pentanedioic acid, dimethyl ester                       |
| 15   | Pentanedioic acid, 2-methyl-, dimethyl ester            |
| 26   | Nonanedioic acid, dimethyl ester                        |
| FAME C8  | Octanoic acid, methyl ester                             |
| FAME C12   | Decanoic acid, methyl ester                             |
| FAME C12   | Dodecanoic acid, methyl ester                           |
| FAME C14   | Methyl tetradecanoate                                   |
| FAME C15 <i>iso</i>  | Isopentadecanoic acid                                   |
| FAME C15   | Pentadecanoic acid, methyl ester                        |
| FAME C15 br.   | Tetradecanoic acid, 12-methyl-, methyl ester            |
| FAME C16 br.   | Tridecanoic acid, 4,8,12-trimethyl-, methyl ester       |
| FAME C16   | Pentadecanoic acid, 14-methyl-, methyl ester            |
| FAME C17 br.   | Hexadecanoic acid, 15-methyl-, methyl ester             |
| FAME C17   | Heptadecanoic acid                                      |
| FAME C18   | Octadecanoic acid, methyl ester                         |
| FAME C20   | Eicosanoic acid, methyl ester                           |
| FAME C22   | Docosanoic acid, methyl ester                           |
| FAME C24   | Tetracosanoic acid, methyl ester                        |
| FAME C26   | Hexacosanoic acid, methyl ester                         |
| FAME C28   | Octacosanoic acid, methyl ester                         |
| FAME C30   | Tricontanoic acid, methyl ester                         |
| FAME C32   | Dotriacontanoic acid, methyl ester                      |

Table 5 (continued)

| <i>Nitrogen-containing compounds</i> |  |
|--------------------------------------|--|
| 28                                   | 2-Methyl,1H-isoindole-1,3-dione                            |
| 10                                   | 2,5-Pyrrolidinedione, 1-methyl-                            |
| 11                                   | 4,4,6-Trimethyl-2-amino(imino)-5,6-dihydro-(4H)1,3-oxazine |
| 17                                   | 2,5-Dimethyl-1-propylpyrrole                               |
| 18                                   | 1-Piperidinecarboxaldehyde                                 |
| 22                                   | 2,5-Pyrrolidinedione, 3-ethyl-1,3-dimethyl-                |
| 23                                   | 4(3H)-Pyrimidinone, 2,3,6-trimethyl-                       |
| 24                                   | 4(1 H)-Pyridinone, 1,2,6-trimethyl-                        |
| 30                                   | 3-Ethyl,2,6-piperidinedione                                |
| 31                                   | 3-Ethyl-1,3-dimethyl pyrrolidinedione                      |
| 33                                   | 4,5-Dimethyl-2-isopropyl oxazole                           |
| <i>Non-lignin aromatic compounds</i> |  |
| 3                                    | Benzaldehyde   |
| 4                                    | Benzene, (methoxymethyl)-                                  |
| 9                                    | Benzoic acid, methyl ester                                 |
| 13                                   | Benzene, 1,4-dimethoxy-                                    |
| 14                                   | Benzenecetic acid, methyl ester                            |
| 20                                   | Benzenepropanoic acid, methyl ester                        |
| 21                                   | Benzoic acid, 2,4-dimethyl-, methyl ester                  |
| 25                                   | 1,2,4-Trimethoxybenzene                                    |
| 27                                   | 2,5-Dimethoxy-4-ethylbenzaldehyde                          |
| 29                                   | 4-Hexylanisole   |
| <i>Other lipid-derived compounds</i> |  |
| 1                                    | Propane, 1,2,3-trimethoxy-                                 |
| 16                                   | 2-Pentanol, 3-ethyl-2-methyl-                              |
| 19                                   | 1-Propanol, 3-methoxy-2, 2-bis(methoxymethyl)-             |
| 32                                   | 2,2-Bis(methoxymethyl)-3-methoxy-1-propanol                |

FAME = fatty acid methyl ester, G = guaiacyl, P = *p*-hydroxyphenyl, S = syringyl.

The levels of total PAHs obtained for the Paleta Creek site were intermediate between Baltimore Harbor and Xiamen Harbor, China. The PAH levels at the contaminated site were, however, higher than those measured in the open seas such as in the Adriatic Sea (12–174  $\mu\text{g kg}^{-1}$ , Marcomini et al., 1986), and Eastern Mediterranean (15–159  $\mu\text{g kg}^{-1}$ , Gogou et al., 2000). PAHs enter the marine environment through aquatic as well as atmospheric pathways. PAHs are derived from several different sources and could be either petrogenic, pyrolytic or biogenic. The predominance of PAHs with molecular weights greater than 202 amu are indicative of a pyrolytic input from pyrolysis of fossil fuels (Lafamme and Hites, 1978), whereas low molecular weight PAHs (one to three rings) are generally obtained from incomplete combustion of fossil fuels or from spillage and disposal of oil or petroleum products (petrogenic). However, the latter are easier to degrade through a combination of physicochemical and biological

processes (Simo et al., 1997). Ratios such as phenanthrene/anthracene and fluoranthene/pyrene have been used in order to distinguish between PAHs of different origins (Gschwend and Hites, 1981). Low phenanthrene/anthracene ratios (<15) (Wise et al., 1988) and high fluoranthene/pyrene ratios (>1) (Sicre et al., 1987) reported here suggests that the PAHs may be produced by the high-temperature pyrolytic processes occurring during combustion of fossil fuels from ships coming to the area.

In both sites the PAH concentration in the surface layer was significantly higher than in the bottom layer. This phenomenon can be due to any or a combination of the following: recent contamination of the surface layer; biodegradation of contaminants in the deeper layers; and sorption onto the  $S_D$  OM in the top layer.

The  $^{13}C$ -NMR spectra of the San Diego sediments exhibited higher aromaticity as compared to a predominantly aliphatic structure, characteristic of marine sediments (Hatcher et al., 1983a; Hedges and Oades, 1997; Zegouagh et al., 1999). A typical NMR spectrum of a marine sediment exhibits a major peak in the paraffinic region which accounts for 50% of the total carbon, with the rest of the carbon being equally distributed among aromatic, carbohydrate, and carboxyl structures (Hedges and Oades, 1997). The high aliphaticity of  $S_D$  OM was attributed to high contribution of aliphatic residues from algal activity. The algal biopolymer algaenan is resistant to biodegradation and is often preserved in the sediment with minor alterations (Hatcher et al., 1983b). The NMR spectra indicated that in addition to their aliphatic nature, they also contain 23–30% of aromatic carbon and relatively high level of carbohydrates (Table 4). Therefore, the resulting  $^{13}C$ -NMR spectra were similar to those obtained for soil OM, rather than typical  $S_D$  OM (Hedges and Oades, 1997). Snape et al. (1989) have shown that the precision of measurements in solid-state CPMAS NMR experiments is of the order of 1–2%. This reproducibility was seen in coal samples even in independent measurements in different laboratories at two different fields, and is expected to be true for high OM samples like the ones under study in this paper.

The high aromatic content exhibited in the NMR spectra was not as a result of contamination from aromatic organic compounds, since such compounds were removed by the initial lipid extraction prior to analysis by NMR. Furthermore, no residues of either any of the PAHs, or their degradation products were detected in the Py-GC/MS or TMAH analyses. Therefore, the high aromaticity of the studied samples is likely due to high input of terrestrial OM. Kokinos et al. (1998) determined that the cell walls of marine dinoflagellate cysts contain relatively condensed, predominantly aromatic structures. However, it is unlikely that these could have significantly contributed to the aromaticity of the San Diego Bay  $S_D$  OM, due to their

low concentrations and their seasonal nature. NMR spectra containing characteristic lignin peaks (147 and 56 ppm) suggest contribution of compounds derived from lignin, which is solely derived from terrestrial vascular plants.

The aliphatic carbon regions in the NMR spectra were dominated by the 30 ppm peak, which had a shoulder at 29 ppm (polymethylene  $(CH_2)_n$  chains). Recently, Hu et al. (2000) suggested that such peaks could be assigned to crystalline and non-crystalline (mobile) parts of the polymethylenic chains. In  $S_D$  OM these polymethylenic structures are generally associated with carbohydrates, proteins, and carboxylic acid functionalities.

Pyrolysis has been proved to be a reproducible technique for analyzing samples of natural OM. Its reproducibility has been demonstrated in the analysis of woody peats (Durig et al., 1989), lignin and carbohydrates (Kleen et al., 1993), and kerogens (Skjevrak et al., 1994). We expect the technique to be reproducible for high OM samples like the ones under study in this paper.

The Py-GC/MS data clearly indicated a higher contribution of lignin-derived residues to the  $S_D$  OM from the Paleta Creek site, as compared to the Coronado Cayes site. This is probably from discharge of a creek containing OM from terrestrial sources to the Paleta Creek site. Lignin-derived monomers were identified as being primarily of the guaiacyl type, suggesting that either the lignin was derived mainly from gymnosperms, or the syringyl lignin units of source plants have been selectively degraded. The only lignin-derived compound identified in the Py-GC/MS chromatograms in the Coronado Cayes samples was phenol (LG1; Fig. 3). But, phenol can also be generated as a pyrolysis product of polyphenolic compounds such as phlorotannins, which are produced by brown macroalgae (Ragan and Glombitza, 1986; van Heemst et al., 1996). It has also been suggested that such products may be derived from melanoidin-type components (Peulve et al., 1996) and amino acids such as tyrosine. Therefore, we conclude that the phenol present in the Coronado Cayes samples is probably not derived from lignin.

In addition to phenol, Py-GC/MS chromatograms exhibit protein-derived materials such as pyrroles, indoles, imidazoles, pyridines, amides, and nitriles. The indoles can originate from tryptophan-containing peptides, whereas the pyrroles can be derived from proline-containing peptides (Tsuge and Matsubara, 1985). The Coronado Cayes surface sediment samples have a higher concentration of protein-derived compounds, suggesting the presence of degraded proteinaceous material from autochthonous sources (algae, bacteria) and/or sewage.

*n*-Alkanes and *n*-alkenes ( $C_8$ – $C_{31}$ ) were detected by Py-GC/MS in all four samples (Fig. 6). These com-

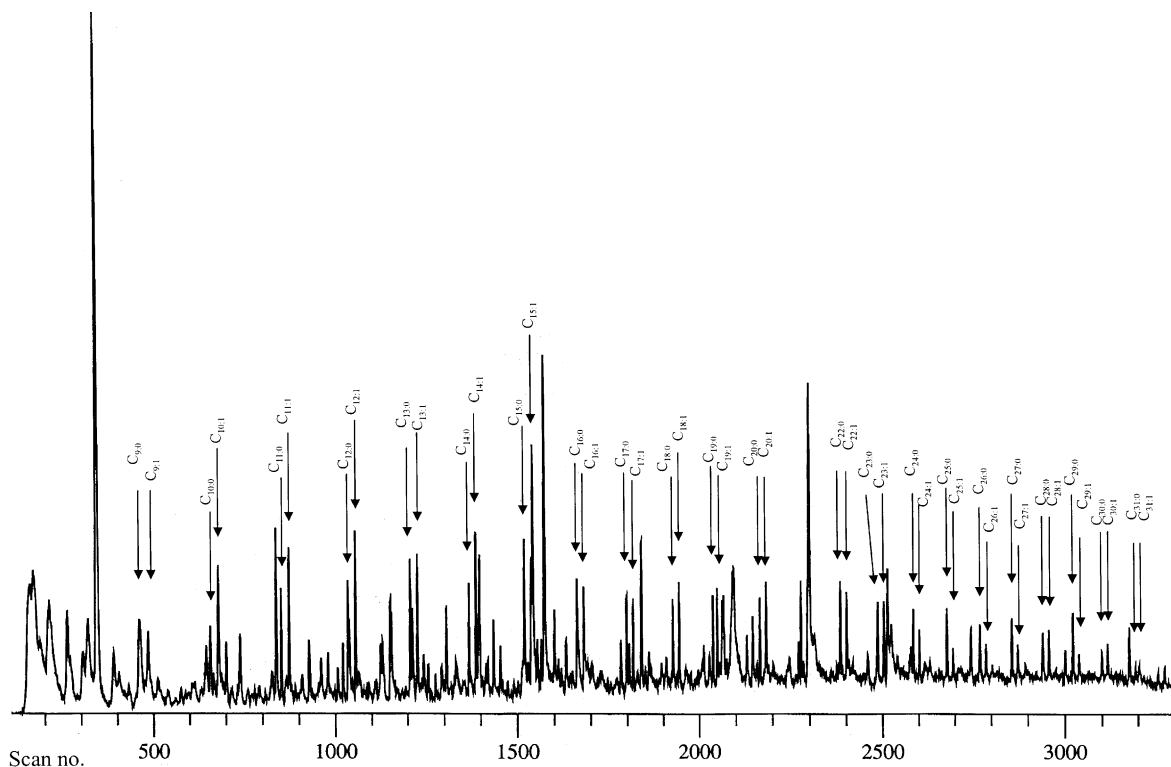


Fig. 6. Py-GC/MS selective ion chromatogram (69+71) of the PCT sample.  $C_{n,0} = n$ -alkane  $C_{n,1} = 1$ -alkene.

pounds are known to derive from algaenan (Largeau et al., 1984), cutan and suberan (Tegelaar et al., 1989), but are more likely derived from algaenan in these settings. A decrease in the concentration of fatty acids with depth was observed in the pyrolyzates obtained from the Coronado Cayes samples suggesting the presence of relatively higher carboxylated material in the top layer. Similar observations were reported in sediments for the Mediterranean Sea (Peulve et al., 1996).

The strong predominance of toluene over other alkylated benzenes in the pyrolysis chromatograms is consistent with other studies of non-contaminated  $S_D$ OM (Peulve et al., 1996). The presence of a major styrene peak in the chromatograms of the Paleta Creek samples implies an anthropogenic input such as from polystyrene waste. However, styrene is also known to be a pyrolysis product of peat (van Smeerdijk and Boon, 1987), suggesting a marker for degraded lignin. Therefore, the origin of styrene in the Paleta Creek site, which has both terrestrial and contaminant input, is unknown.

Several other di- and trialkylated benzenes were detected among the pyrolyzates. These compounds have been considered as originating from  $\beta$ -cleavage of aromatic rings linked via alkyl chains to the macromolecular structure (Hartgers et al., 1994). But these compounds could also be formed due to cyclization, or

aromatization processes occurring during pyrolysis (Zegouagh et al., 1999). Since the NMR spectra also point towards high aromaticity, we believe that these compounds are derived from the  $S_D$ OM macromolecular structures. Various alkylated phenols (2- and 3-methyl, and dimethyl phenols) were present only in the samples from Coronado Cayes. These samples contained low terrestrial OM residue, and therefore suggest that the alkylated phenols might be derived from tyrosine.

The pyrolyzates showed different derivatives of thiophene, which are difficult to assign to any particular group of precursors. However, sulfate-reducing bacteria in such anoxic environments produce sulfides and disulfides which are expected to cross-link with the functionalized lipids and other biochemicals, and get incorporated in the macromolecular matrix, much like in the vulcanization process (Schmid et al., 1987). It is believed, that the thiophenes are generated as a result of pyrolyzing such sulfur-containing bonds.

TMAH thermochemolysis-GC/MS has been proved to be useful for obtaining structural information of terrestrial markers like lignin in marine sediments. The Paleta Creek site yielded higher levels of compounds derived from lignin as compared to the sample from the Coronado Cayes site. This finding supports the

$^{13}\text{C}$ -NMR and Py-GC/MS data suggesting a higher terrestrial input to the Paleta Creek site. The major lignin-derived peaks were G-type compounds, (G1, G3, G4, G5, G6, G10, G21, and G22), suggesting input from gymnosperms. This finding indicates that although both the sites are very close to the shore, the  $\text{S}_\text{D}$ OM from the Paleta Creek site is more characteristic of terrestrial OM.

The TMAH thermochemolysis yielded several FAME peaks, with the  $\text{C}_{16}$  and  $\text{C}_{18}$  being the most intense. In this procedure, FAMES are generally formed as a result of transesterification of triglycerides and other lipids (Challinor, 1991). Marine sediments from productive systems can contain a substantial amount of fatty acids (mainly  $\text{C}_{16}$  and  $\text{C}_{18}$ ) with a predominance of even-numbered fatty acids (Parkes, 1987). Odd carbon-numbered and branched-chain fatty acids are commonly used as bacterial biomarkers (Parkes, 1987). Fatty acids having more than 24 carbon atom chains were reported to be characteristic of terrestrial OM (Boon and Duinveld, 1996). The Coronado Cayes sample did not show significant peaks of FAMES having more than 24 carbon atoms, suggesting a low terrestrial input to this site. However, their concentration was higher in the Coronado Cayes samples than in the more terrestrial Paleta Creek samples and so they must have been derived from other sources.

## 5. Conclusions

In this study we have analyzed the chemical composition of  $\text{S}_\text{D}$ OM from two sites (contaminated and pristine) in the San Diego Bay area using a combination of analytical techniques ( $^{13}\text{C}$  NMR, Py-GC/MS and TMAH thermochemolysis-GC/MS). The PAH concentrations were higher in the surface layer, suggesting that they had been derived from recent contamination, and that PAHs in the deeper layers had been subjected to biodegradation. Predominance of the higher molecular weight PAHs indicates a pyrolytic origin for the PAHs. All chemical analyses indicated that the  $\text{S}_\text{D}$ OM from the studied sites resembled soil OM rather than typical near-shore  $\text{S}_\text{D}$ OM. In addition, the main differences between the  $\text{S}_\text{D}$ OM from the different sites (i.e., contaminated vs. pristine) were related to terrestrial OM input (mainly lignin).

## Acknowledgements

This research was supported with research funding from the Office of Naval Research (ONR) Grant #N00014-99-1-0073 and by postdoctoral award # FI-275-98 from BARD, The US–Israel Binational Agricultural Research and Development Fund.

## References

- Ashley, J.T.F., Baker, J.E., 1999. Hydrophobic organic contaminants in surficial sediments of Baltimore Harbor: Inventories and sources. *Environ. Toxicol. Chem.* 18 (5), 838–849.
- Boon, A.R., Duinveld, G.C.A., 1996. Phytopigments and fatty acids as molecular markers for the quality of near bottom particulate organic matter in the North Sea. *J. Sea Res.* 35, 279–291.
- Carter, W., Suffet, I., 1982. Binding of DDT to dissolved humic materials. *Environ. Sci. Technol.* 16, 735–740.
- Challinor, J.M., 1991. The scope of pyrolysis/methylation reactions. *J. Anal. Appl. Pyrolysis* 20, 15–24.
- Challinor, J.M., 1996. A rapid simple pyrolysis derivatization gas chromatography–mass spectrometry for profiling of fatty acids in trace quantities of lipids. *J. Anal. Appl. Pyrolysis* 37, 185–197.
- Chefetz, B., van Heemst, J.D.H., Chen, Y., Romaine, C.P., Chorover, J., Rosario, R., Guo, M., Hatcher, P.G., 2000. Organic matter transformation during the weathering process of spent mushroom substrate. *J. Environ. Qual.* 29, 592–602.
- Clifford, D.J., Carson, D.M., McKinney, D.E., Bortiatynski, J.M., Hatcher, P.G., 1995. A new rapid technique for the characterization of lignin in vascular plants: thermochemolysis with tetramethylammonium hydroxide (TMAH). *Org. Geochem.* 23, 169–175.
- Coates, J.D., Woodward, J., Allen, J., Philp, P., Lovley, D.R., 1997. Anaerobic degradation of polycyclic aromatic hydrocarbons and alkanes in petroleum-contaminated marine harbor sediments. *Appl. Environ. Microbiol.* 63 (9), 3589–3593.
- del Rio, J.C., McKinney, D.E., Knicker, H., Nanny, M.A., Minard, R.D., Hatcher, P.G., 1998. Structural characterization of bio- and geo-macromolecules by off-line thermochemolysis with tetramethylammonium hydroxide. *J. Chromatogr. A* 823, 433–448.
- Durig, J.R., Calvert, G.D., Esterle, J.S., 1989. Development of a pyrolysis–gas chromatographic–Fourier transform infrared spectroscopic technique for the study of woody peats. *J. Anal. Appl. Pyrolysis* 14 (4), 295–308.
- Ergin, M., Gaines, A., Galletti, G.C., Chiavari, G., Fabbri, D., Yucesoy-Eryilmaz, F., 1996. Early diagenesis of organic matter in recent Black Sea sediments: Characterization and source assessment. *Appl. Geochem.* 11, 711–720.
- Fabbri, D., Helleur, R., 1999. Characterization of the tetramethylammonium hydroxide thermochemolysis products of carbohydrates. *J. Anal. Appl. Pyrolysis* 49, 277–293.
- Filley, T.R., Minard, R.D., Hatcher, P.G., 1999. Tetramethylammonium hydroxide (TMAH) thermochemolysis: Proposed mechanisms based upon the application of  $^{13}\text{C}$  labeled TMAH to synthetic model lignin dimer. *Org. Geochem.* 30, 607–621.
- Flegal, A.R., Sanudo-Wilhelmy, S.A., 1993. Comparable levels of trace metal contamination in two semi-enclosed embayments: San Diego Bay and South San Francisco Bay. *Environ. Sci. Technol.* 27, 1934–1936.
- Garcia, B., Mogollon, J.L., Lopez, L., Rojas, A., Bifano, C., 1994. Humic and fulvic acid characterization in sediments from a contaminated tropical river. *Chem. Geol.* 118, 271–287.

- Gelin, F., Boogers, I., Noordeoos, A.A.M., Damste, J.S.S., Hatcher, P.G., De Leeuw, J.W., 1996. Novel, resistant microalgal polyethers: An important sink of organic carbon in the marine environment. *Geochim. Cosmochim. Acta* 60, 1275–1280.
- Gogou, A., Bouloubassi, I., Stepahnou, E.G., 2000. Marine organic geochemistry of the eastern Mediterranean: I. Aliphatic and polyaromatic hydrocarbons in Cretan Sea surficial sediments. *Mar. Chem.* 68, 265–282.
- Gschwend, P.M., Hites, R., 1981. Fluxes of the polycyclic aromatic hydrocarbons to marine and lacustrine sediments in the northeastern United States. *Geochim. Cosmochim. Acta* 45, 2359–2367.
- Hartgers, W.A., Sinninghe Damste, J.S., Requejo, A.G., Allan, J., Hayes, J.M., Ling, Y., Xie, T.M., Primach, J., de Leeuw, J.W., 1994. Evidence for only minor contribution from bacteria to sedimentary organic carbon. *Nature* 369, 224–227.
- Hatcher, P.G., Breger, I.A., Dennis, L.W., Maciel, G.E., 1983a. Solid-state  $^{13}\text{C}$  NMR of sedimentary humic substances: New revelations on their chemical composition. In: Gjesing, E.T., Christman, R.F. (Eds.), *Aquatic and Terrestrial Humic Materials*. Ann Arbor Science Publishers, Ann Arbor, USA, pp. 37–82.
- Hatcher, P.G., Clifford, D.J., 1994. Flash pyrolysis and in situ methylation of humic acids from soil. *Org. Geochem.* 21, 1081–1092.
- Hatcher, P.G., Nanny, M.A., Minard, R.D., Dible, S.D., Carson, D.M., 1996. Comparison of two thermochemolytic methods for the analysis of lignin in decomposing gymnosperm wood: The CuO oxidation method and the method of thermochemolysis with tetramethylammonium hydroxide (TMAH). *Org. Geochem.* 23, 881–888.
- Hatcher, P.G., Rowan, R., Mattingly, M.A., 1980.  $^1\text{H}$  and  $^{13}\text{C}$  NMR of marine humic acids. *Org. Geochem.* 2, 77–85.
- Hatcher, P.G., Spiker, E.C., Szeverenyi, N.M., Maciel, G.E., 1983b. Selective preservation and origin of petroleum-forming aquatic kerogen. *Nature* 305, 498–501.
- Hedges, J.I., Mann, D.C., 1979. The lignin geochemistry of marine sediments from the southern Washington coast. *Geochim. Cosmochim. Acta* 43, 1809–1818.
- Hedges, J.I., Oades, J.M., 1997. Comparative organic geochemistries of soils and marine sediments. *Org. Geochem.* 27, 319–361.
- Hediger, S., Meier, B.H., Ernst, R.R., 1993. Cross polarization under fast magic angle sample spinning using amplitude modulated spin-lock sequences. *Chem. Phys. Lett.* 213 (5–6), 627–635.
- Hu, W.G., Jingdong, M., Xing, B., Schmidt-Rohr, K., 2000. Poly(methylene) crystallites in humic substances detected by nuclear magnetic resonance. *Environ. Sci. Technol.* 34, 530–534.
- Huggett, R.J., Van Veld, P.A., Smith, C.L., Hargis Jr., W.J., Vogelbein, W.K., Weeks, B.A., 1992. The effects of contaminated sediments in the Elizabeth River. In: Burton Jr., G.A. (Ed.), *Sediment Toxicity Assessment*. Lewis, Boca Raton, FL, pp. 403–430.
- Kleen, M., Lindblad, G., Backa, S., 1993. Quantification of lignin and carbohydrates in kraft pulps using analytical pyrolysis and multivariate data analysis. *J. Anal. Appl. Pyrolysis* 25, 209–227.
- Kokinos, J.P., Eglinton, T.I., Goni, M.A., Boon, J.J., Martoglio, P.A., Anderson, D.M., 1998. Characterization of a highly resistant biomacromolecular material in the cell wall of a marine dinoflagellate resting cyst. *Org. Geochem.* 28 (5), 265–288.
- Laflamme, R.E., Hites, R.A., 1978. The global distribution of polycyclic aromatic hydrocarbons in recent sediments. *Geochim. Cosmochim. Acta* 42, 289–303.
- Largeau, C., Casadevall, E., Kadouri, A., Metzger, P., 1984. Formation of a *Botryococcus*-derived kerogens. Comparative study of immature Torbanite and the extant alga *Botryococcus braunii*. In: Shenck, P.A., et al. (Eds.), *Advances in Organic Geochemistry*. Pergamon Press, Oxford, UK, pp. 327–332.
- Lenihan, H.S., Oliver, J.S., Stephenson, M.A., 1990. Changes in hard bottom communities related to boat mooring and tributyltin in San Diego Bay: A natural experiment. *Mar. Ecol. Prog. Ser.* 60, 147–159.
- Marcomini, A., Pavoni, B., Donazzolo, R., Orto, A.A., 1986. Combined preparative and analytical use of normal phase and reversed phase high performance liquid chromatography for the determination of aliphatic and polycyclic aromatic hydrocarbons in sediments of the Adriatic Sea. *Mar. Chem.* 18, 71–84.
- McCain, B.B., Chan, S.L., Krahn, M.M., Brown, D.W., Myers, M.S., Landahl, J.T., Pierce, S., Clark Jr., R.C., Varanasi, U., 1992. Chemical contamination and associated fish diseases in San Diego Bay. *Environ. Sci. Technol.* 26 (4), 725.
- McKinney, D.E., Bortiatynski, J.M., Carson, D.M., Clifford, D.J., de Leeuw, J.W., Hatcher, P.G., 1996. Tetramethylammonium hydroxide (TMAH) thermochemolysis of the aliphatic biopolymer cutan: Insights into the chemical structure. *Org. Geochem.* 24, 641–650.
- McKinney, D.E., Hatcher, P.G., 1996. Characterization of peatified and coalified wood by tetramethylammonium hydroxide (TMAH) thermochemolysis. *Int. J. Coal Geol.* 32, 217–228.
- Parke, R.J., 1987. Analysis of microbial communities within sediments using biomarkers. In: *Ecology of Microbial Communities*. SGM 41, Cambridge University Press, Cambridge, UK, pp. 147–177.
- Peulve, S., de Leeuw, J.W., Sicre, M.A., Baas, M., Saliot, A., 1996. Characterization of macromolecular organic matter in sediment traps from the northwestern Mediterranean Sea. *Geochim. Cosmochim. Acta* 60, 1239–1259.
- Pouwels, A.D., Eijkel, G.B., Boon, J.J., 1989. Curie-point pyrolysis–capillary gas chromatography–high resolution mass spectrometry of microcrystalline cellulose. *J. Anal. Appl. Pyrolysis* 14, 237–280.
- Pulchan, J., Abrajano, T.A., Helleur, R., 1997. Characterization of tetramethylammonium hydroxide thermochemolysis products of near-shore marine sediments using gas chromatography/mass spectrometry and gas chromatography/c combustion/isotope ratio mass spectrometry. *J. Anal. Appl. Pyrolysis* 42, 135–150.
- Ragan, M.A., Glombitza, K.W., 1986. Phlorotannins brown algal polyphenols. *Prog. Phycol. Res.* 4, 129–241.
- Schmid, J.C., Connan, J., Albrecht, P., 1987. Occurrence and geological significance of long-chain dialkylthiacyclopentanes. *Nature* 329, 54–56.
- Sicre, M.A., Marty, J.C., Saliot, A., Aparicio, X., Grimalt, J., Albaiges, J., 1987. Aliphatic and aromatic hydrocarbons in

- different sized aerosols over the Mediterranean Sea: Occurrence and origin. *Atmos. Environ.* 21, 2247–2259.
- Simo, R., Grimalt, J.O., Albaiges, J., 1997. Loss of unburned-fuel hydrocarbons from combustion aerosols during atmospheric transport. *Environ. Sci. Technol.* 31, 2697–2700.
- Skjevrak, I., Larter, S., Van Graas, G., Jones, M., Berge, E., 1994. A practical approach to quantitative group type analysis of kerogens using non-dedicated pyrolysis–mass spectrometry equipment: Applications and comparison with other methods. *Org. Geochem.* 22 (3–5), 873–883.
- Snape, C.E., Axelson, D.E., Botto, R.E., Delpuech, J.J., Tekely, P., Gerstein, B.C., Pruski, M., Maciel, G.E., Wilson, M.A., 1989. Quantitative reliability of aromaticity and related measurements on coals by  $^{13}\text{C}$  N.M.R. A debate. *Fuel* 68, 547–560.
- Swift, R., 1996. Organic matter characterization. In: D. Sparks (Ed.), *Methods of Soil Analysis. Part 3. Chemical Methods*, SSSA Book Series No. 5. Soil Science Society of America, Madison, WI, USA, pp. 1011–1069.
- Tegelaar, E.W., De Leeuw, J.W., Derenne, S., Largeau, C., 1989. A reappraisal of kerogen formation. *Geochim. Cosmochim. Acta* 53, 3103–3106.
- Tsuge, S., Matsubara, H., 1985. High-resolution pyrolysis–gas chromatography of proteins and related materials. *J. Anal. Appl. Pyrolysis* 8, 49–64.
- Van Der Kaaden, A., Boon, J.J., de Leeuw, J.W., de Lange, F., Wijnand Schuyl, P.J., Schulten, H.R., Bahr, U., 1984. Comparison of analytical pyrolysis techniques in the characterization of chitin. *Anal. Chem.* 56, 2160–2164.
- van Smeerdijk, D.G., Boon, J.J., 1987. Characterization of subfossil Sphagnum leaves, rootlets of Ericaceae and their peat by pyrolysis–high resolution gas chromatography–mass spectrometry. *J. Anal. Appl. Pyrolysis* 11, 377–402.
- Vandenbroucke, M., Pelet, R., Debyser, Y., 1985. Geochemistry of humic substances in marine sediments. In: Aiken, G.M., McKnight, D.M., Wershaw, R.L. (Eds.), *Humic Substances in Soil, Sediment, and Water*. Wiley Interscience, New York, pp. 249–273.
- van Heemst, J.D.H., Peulve, S., de Leeuw, J.W., 1996. Novel algal polyphenolic biomacromolecules as significant contributors to resistant fractions of marine dissolved and particulate organic matter. *Org. Geochem.* 24, 629–640.
- Wise, S.A., Benner, B.A., Byrd, G.D., Chesler, S.N., Rebbert, R.E., Schantz, M.M., 1988. Determination of polycyclic aromatic hydrocarbons in a coal tar standard reference material. *Anal. Chem.* 60, 887–894.
- Zegouagh, Y., Derenne, S., Largeau, C., Bertrand, P., Sicre, M., Saliot, A., Rousseau, B., 1999. Refractory organic matter in sediments from the northwest African upwelling system: Abundance, chemical structure and origin. *Org. Geochem.* 30, 83–99.
- Zeng, E.Y., Vista, C.L., 1997. Organic pollutants in the coastal environment off San Diego, California. 1. Source identification and assessment by compositional indices of polycyclic aromatic hydrocarbons. *Environ. Toxicol. Chem.* 16 (2), 179–188.
- Zhou, J.L., Hong, H., Zhang, Z., Maskaoui, K., Chen, W., 2000. Multi-phase distribution of organic micropollutants in Xiamen Harbour, China. *Water Res.* 34 (7), 2132–2150.
- Zirino, A., Belli, S.L., Van Der Weele, D.A., 1998. Copper concentration and Cu(II) activity in San Diego Bay. *Electroanalysis* 10 (6), 423–427.